

Focused Research on Time Reversal Method for Ultrasonic Guided Waves

Junbin Duan
Yangtze University
School of Electronics
Information and Electrical
Engineering
Jingzhou, Hubei, China

Peng Zheng
Yangtze University
School of Electronics
Information and Electrical
Engineering
Jingzhou, Hubei, China

Chen Cai
Yangtze University
School of Electronics
Information and Electrical
Engineering
Jingzhou, Hubei, China

Abstract: Ultrasonic guided wave inspection is widely applied in pipeline health monitoring due to its long propagation distance, high efficiency, and suitability for large-scale monitoring. However, dispersion effects and multimode coupling characteristics during guided wave propagation cause echo signal energy dispersion, reducing detection sensitivity for minute defects. The time reversal method enhances defect echo signals by inverting received signals. This study employs COMSOL simulations to analyze the impact of different truncation window widths on time reversal focusing performance. Results indicate that increasing the truncation window width captures more guided wave mode information, significantly enhancing defect echo energy. The defect reflection coefficient improved from 0.3158 to 0.3653, with energy amplification increasing from $2.141\times$ to $2.478\times$. The study demonstrates that appropriately selecting the truncation window width enhances focusing performance, providing theoretical support for parameter optimization of the time reversal method in pipeline defect detection.

Keywords: Ultrasonic guided wave; Time reversal; Pipeline inspection; Weld defects; Truncation window; Numerical simulation

1. INTRODUCTION

In recent years, accelerated industrialization has spurred extensive global research on structural health monitoring (SHM)[1-4]. Pipelines, as critical infrastructure for transporting petroleum, natural gas, and chemical energy, are prone to damage such as corrosion, cracks, and weld defects during long-term service [5–8]. Consequently, developing efficient and reliable non-destructive testing (NDT) techniques for pipeline health monitoring holds significant importance [9–10].

Ultrasonic guided wave testing technology has gained extensive application in pipeline structural health monitoring due to its ability to propagate along structures over long distances and enable large-scale inspection. Joseph L. Rose systematically investigated the propagation mechanisms of ultrasonic guided waves in solid structures, establishing a comprehensive theoretical framework for guided waves. His research summarized the propagation characteristics of different guided wave modes in plate and pipeline structures, laying a crucial theoretical foundation for the advancement of guided wave NDT technology [11]. Subsequently, D. N. Alleyne and Peter Cawley addressed the challenge of identifying multimodal guided wave signals by proposing a guided wave signal analysis method based on the two-dimensional Fourier transform. This approach effectively separates signals from different modes, thereby enhancing the analytical capability of guided wave propagation characteristics [12]. Building upon this, Michael J. S. Lowe investigated the propagation patterns of guided waves within pipeline structures for defect detection. His research demonstrated that guided waves enable long-distance detection and can effectively identify corrosion and crack defects in pipelines [13]. Additionally, Peter D. Wilcox addressed the low efficiency of large-scale structural inspections by proposing a method for guided wave structural health monitoring using permanently installed sensors. This approach enables long-term online monitoring of structures, further advancing the

application of guided wave detection technology in engineering structures [14].

To enhance the signal resolution capability of guided wave detection, researchers introduced time reversal techniques into this field. Mathias Fink proposed the theory of time-reversed acoustics to address the difficulty of focusing wave fields in complex media. Studies demonstrated that by performing time inversion on received signals and re-exciting them, adaptive focusing of the wave field at the original scattering source location can be achieved [15]. Subsequently, Claude Prada conducted further research on time-reversal mirror technology to address acoustic wave propagation focusing. His work validated the superior wavefield focusing capability of time-reversal methods in complex media [16]. Concurrently, James E. Michaels applied time-reversal techniques to guided wave detection for structural damage localization. Results demonstrated this method significantly enhances the accuracy of structural damage localization [17]. Additionally, Victor Giurgiutiu investigated guided wave damage detection using piezoelectric sensors for structural health monitoring. His work advanced the application of guided wave detection in engineering structural health monitoring [18]. Although time reversal techniques significantly enhance the signal focusing capability of guided wave detection, their focusing effectiveness remains influenced by signal processing parameters in practical applications. Among these, the time-intercept window width directly impacts the integrity of defect signal information. An excessively narrow window may result in partial loss of defect information, while an overly wide window may introduce additional noise, thereby compromising focusing performance. Therefore, investigating the impact of time-interpolation window parameters on time-reversal guided wave detection performance is crucial. This paper establishes a pipeline model containing weld defects using COMSOL finite element software. Through numerical simulation, it analyzes the variation patterns of time-reversal guided wave focusing effects under different window width conditions, providing reference for optimizing time-reversal parameters.

1.1 Focusing Characteristics of Time Reversal Method in Pipelines

In pipeline defect detection, ultrasonic guided waves encounter sudden cross-sectional changes (e.g., corrosion thinning or deposit thickening) along their propagation path, triggering reflection and modal conversion phenomena. The characteristics of reflected waves are determined by the defect's geometric features. As passive wave sources, defects modulate the modal composition and energy distribution of reflected waves through their morphology. Traditional single-mode guided wave detection methods, constrained by dispersion effects and multimode interference (e.g., longitudinal-to-bending mode conversion), can only identify defects of significant dimensions, leaving detection blind spots for micro-scale damage. Time reversal technology overcomes this limitation through a dual domain (spatiotemporal) focusing mechanism: First, the optimized selection of the time reversal window must fully encompass the time frequency characteristics of the defect echo to ensure the completeness of defect information captured. Second, time-reversal excitation employs phase-conjugate reconstruction of the wavefield to create an energy-focusing effect at defective locations, significantly suppressing energy attenuation and modal overlap caused by dispersion. This method enhances the distinguishability of reflection signals from minute defects and improves localization accuracy through wave packet compression and energy concentration, providing a highly sensitive and robust interference-resistant solution for pipeline structural health monitoring.

1.1.1 Focusing on the Process of Time Reversal Method

The time-reversal focusing method for pipeline guided ultrasonic waves is based on the time-reversal symmetry of the guided wave equation and the principle of acoustic field reciprocity. In this method, the time-domain signals received by each sensor are sampled with a fixed window width τ , time-reversed, and then re-excited into the pipeline by the corresponding sensors in synchronization. According to time-reversal theory, the re-excited signals achieve wavefield reconstruction and energy focusing at the original defect location. Affected by the dispersion characteristics of guided waves, multimodal echo signals arrive at the receiver sequentially according to their group velocity differences. This causes time-domain waveform broadening and energy dispersion, thereby weakening the amplitude characteristics of defect echoes. The time reversal method achieves time-domain inversion of the received signal, enabling slower modes to be re-excited first and faster modes later. By leveraging the consistency of propagation delays across all modes after inversion, it facilitates simultaneous superposition at the defect location, creating a time-focusing effect. This concentrates and amplifies multi-mode energy at weld defects. The general workflow of time reversal is as follows: First, select an appropriate excitation signal and center frequency, then apply an excitation voltage at the pipe end to stimulate the L(0,2) guided wave mode. Subsequently, collect the guided wave signal reflected by the defect at the receiver end, which contains defect related modal information. By analyzing the reflected signal to extract defect characteristics and calculate the reflection coefficient, the excitation signal is combined with the reflected signal and amplified through a feedback mechanism. Finally, the feedback signal is processed to obtain the reflection detection results, enabling precise localization and evaluation of pipeline defects.

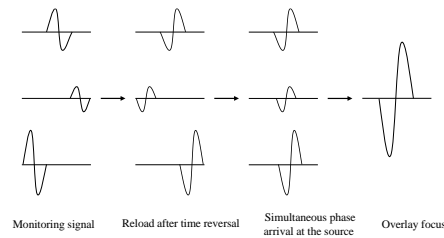


Fig. 1 Focusing Process Diagram of the Time Reversal Method

1.1.2 Spatial Focusing Characteristics of the Time Reversal Method

The spatial focusing capability of the time reversal method stems from the time-reversal symmetry of the wave equation. The scattered wavefront received by the sensor array undergoes time-domain inversion before being re-injected into the medium. The propagating wavefield then achieves phase matching at the original scattering source, enabling adaptive energy convergence based on the principle of reciprocity. This process essentially utilizes wavefield reconstruction to perform inverse compensation for the propagation path, thereby forming a focal point at the target location.

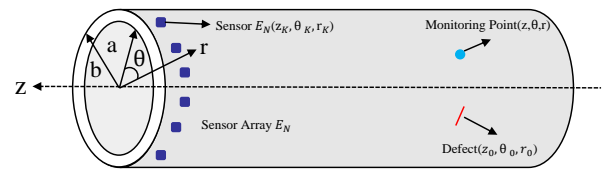


Fig. 2 Schematic diagram of pipeline coordinates for a single defect

The analysis is based on the pipeline coordinate system shown in Figure. 2, which includes a single defect. Consider multiple excitation sensors arranged circumferentially at equal intervals along the pipeline end, forming a time-reversed sensor array E_N . The column coordinates of any sensor E_K can be expressed as (Z_K, θ_K, r_K) . In ultrasonic guided wave pipeline defect detection, when the sensor array excites a narrowband pulse signal at the center frequency ω_0 , the defect can be treated as an equivalent passive secondary wave source. The resulting guided wave signal can be represented in the frequency domain as:

$$S_{Re}(z, r, \theta, \omega) = G_{Re}(z, r, \theta, \omega)E(\omega) \quad (1)$$

In the above equation, G_{Re} denotes the transfer function from the defect point (Z_K, θ_K, r_K) to the sensor E_K , and $E(\omega)$ represents the Fourier transform result of the defect scattering signal in the frequency domain. Based on the principle of acoustic field reciprocity, time reversal can be achieved by applying a phase conjugate transformation to the received signal and reversing its time sequence to reconstruct the wavefield:

$$S_{TR}(z, r, \theta, \omega) = e^{j\omega\tau}G_{Re}^*(z, r, \theta, \omega)E^*(\omega) \quad (2)$$

where the superscript "*" denotes complex conjugation, and the subscript TR indicates the signal is reconstructed after time inversion. After loading the inverted signal as a secondary

excitation source, the wavefield excited at any spatial monitoring point (Z, θ, r) can be expressed as:

$$S_{TR}(z, r, \theta, \omega) = \sum_{k=1}^N e^{j\omega\tau} G_{Ex} G_{Re}^*(z, r, \theta, \omega) E^*(\omega) \quad (3)$$

where: G_{Ex} is the transfer function from the sensor to the monitoring point. By defining the time-reverse transfer function:

$$G_{TR} = \sum_{k=1}^N e^{j\omega\tau} G_{Ex} G_{Re}^* \quad (4)$$

The total wavefield is:

$$S_{TR} = G_{TR} E^*(\omega) \quad (5)$$

Based on the orthogonal mode expansion theory, the axial displacement expression is:

$$u(z, r, \theta, t) = \sum_{n,m} A_{nm} \cos(n\theta) e^{i(knmz - \omega t)} \quad (6)$$

Through derivation, the time-reversed signal amplitude expression is obtained as:

$$|A_{TR,Max}(z, \theta, r)|^2 = \frac{2\pi B_H^2 |H_{TR}(\omega, z, \theta, r)|^2 |E(\omega)|^2}{\sqrt{1 + B_H^4 \left[\frac{\partial^2 K_{nm}(\omega)}{\partial \omega^2} (z - z_0) \right]^2}} \quad (7)$$

where: B_H denotes the half-bandwidth; K_{nm} represents the wave number of the m th guided wave in the n th mode; $E(\omega)$ is the Fourier transform of the reflected echo signal; $Z = Z_0$ is the axial distance from the defect to the observation point.

Where: B_H denotes the signal's half-bandwidth; K_{nm} represents the wave number corresponding to the n th-order, m th-mode guided wave; $E(\omega)$ is the frequency-domain representation of the defect reflection echo signal after Fourier transform; $Z = Z_0$ defines the axial distance between the defect location and the observation point. The time-reversal transfer function satisfies:

$$|H_{TR}(\omega, z, \theta, r)|^2 = r_0^4 \left\{ \sum_{nm} \left\{ H_{nm}^2 f_n^2(\theta_0) \sum_{k=1}^N \frac{1}{2} [\cos(n\theta_0 - n\theta) + \cos(n(\theta + \theta_0 - 2\theta_k))] \right\} \right\} \quad (8)$$

Regarding the formation mechanism of spatial focusing, when the sensor array achieves sufficient circumferential density such that θ_k traverses the full range from 0 to 2π , the wavefield reconstruction will exhibit excellent spatial resolution. If the

monitoring point and defect share the same circumferential orientation at this point, i.e., $\theta = \theta_0$, the numerator term in equation (7) will approach its peak value. Simultaneously, if the axial coordinate also aligns precisely with the defect location, i.e., $Z = Z_0$, the denominator term in equation (8) will be minimized. The combined effect of these two conditions causes the magnitude of the time-reversal transfer function to reach its global maximum at the defect location, signifying that the wavefield energy achieves spatial convergence at this point. Physically, this focusing effect stems from the phase conjugation operation precisely compensating for propagation path differences. Scattered signals from different paths and modes achieve phase alignment at the defect location after phase rearrangement, forming a coherent superposition that significantly enhances the echo amplitude. For circumferentially uniform sensor arrays, this characteristic manifests as a pronounced signal amplitude at the defect's azimuth, constituting a highly sensitive and directional defect detection mechanism.

1.1.3 Time-Focusing Characteristics of the Time Reversal Method

When ultrasonic guided waves encounter defects in pipelines, their wavefield undergoes complex modal coupling and energy redistribution. The original single incident mode excites a series of new guided wave modes at the defect boundary. These modes, together with the signals directly reflected by the defect, form a multi-component wave packet that propagates along the pipeline and is received by the sensor array deployed at the end. Due to the combined influence of pipeline geometric constraints and material constitutive relationships, the dispersion characteristics of each mode order are determined. The group velocities corresponding to different modal components vary, causing them to arrive at the sensor at different times after traveling the same axial distance. Let the axial distance between the defect and the sensor be z . Analyzing any two modal orders, denote their group velocities as C_{g1} and C_{g2} , with $C_{g1} > C_{g2}$. The accumulated time difference in arrival between the two during propagation can be expressed as:

$$\Delta t = \frac{z}{C_{g2}} - \frac{z}{C_{g1}} \quad (9)$$

After applying time reversal and phase conjugation to the multimode signal collected by the receiving sensor, it is re-excited by loading it onto the corresponding excitation unit. This operation prioritizes excitation of the slower-propagating mode, while delaying excitation of the faster mode by Δt . Following this temporal rearrangement, the arrival times of the two guided modes propagating back from the sensor toward the defect are expressed as:

$$t_1 = \frac{z}{C_{g1}} + \Delta t, t_2 = \frac{z}{C_{g1}} \quad (10)$$

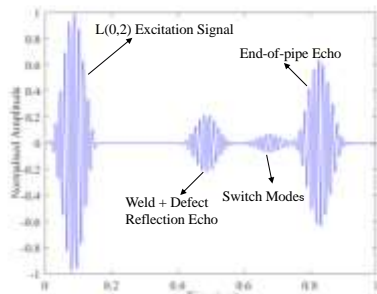
Specifically expressed as:

$$\Delta t_{TR} = t_1 - t_2 = \frac{z}{C_{g1}} + \left(\frac{z}{C_{g2}} - \frac{z}{C_{g1}} \right) - \frac{z}{C_{g2}} = 0 \quad (11)$$

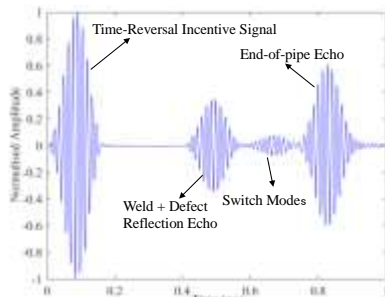
The time reversal method employs a temporal compensation mechanism to prioritize low-velocity modes and delay high-velocity modes, achieving synchronous arrival of multimodal guided waves at the defect site to form a time-focusing effect. This effect effectively suppresses wave packet broadening caused by dispersion, concentrating defect reflection signals in the time domain and thereby enhancing detection capability for minute defects. The defect reflection coefficient is defined as the ratio of the amplitude of the defect reflection echo wave packet to the amplitude of the excitation signal wave packet, i.e.,

$$\text{Defect Reflection Coefficient} = \frac{\text{Defect reflection echo packet peak}}{\text{Peak of the excitation signal packet}} \quad (12)$$

Monitoring the same pipeline weld defect using both direct guided wave and time reversal methods revealed that normalized axial displacement time-history curves demonstrated the time reversal method significantly amplified defect reflection echo amplitude. Calculations showed the defect reflection coefficient for the direct guided wave method was 0.1474, while the time reversal method enhanced it to 0.3158—approximately 2.141 times higher. This result validates the effectiveness of the time reversal method in enhancing defect signal response intensity.



(a) Schematic of direct guided wave time history curve



(b) Schematic of time-reversal method time history curve

Figure 3: 45° defect in the 1100 mm groove-type fillet weld

Applying the time reversal method to guided wave detection of pipeline weld defects leverages its spatiotemporal wavefield

reconstruction and energy focusing mechanism. This enables simultaneous arrival and energy convergence of multimodal guided waves at the defect location. This process manifests temporally as a significant enhancement in defect reflection echo amplitude and spatially as markedly higher energy concentration in the circumferential defect region compared to surrounding areas, forming localized energy accumulation. This energy distribution disparity enables precise circumferential localization of weld defects.

1.2 Correlation Analysis Between Window Width and Inverted Guided Wave Energy

The propagation behavior of guided waves within structures is often simulated using numerical methods, primarily including the finite element method, boundary element method, and finite difference method. Among these, the finite element method, due to its excellent adaptability to geometry and materials, has become the most widely applied simulation technique in this field, enabling observation of ultrasonic guided wave propagation at pipeline welds. Therefore, this chapter employs numerical simulation to investigate the influence of pipeline weld defects with varying time-selective windows on ultrasonic guided waves propagating through pipelines. The energy method is used to calculate the energy values of reflected echoes from weld defects, examining the relationship between different time-reversal selective window widths and the energy focusing capability of weld reflection echoes.

1.2.1 Relationship Between Signal Interception Window and Reflection Coefficient

According to time-reversal wave theory, weld defects can be regarded as secondary passive wave sources under guided wave interaction. When incident waves interact with them, they excite multimodal responses accompanied by dispersion effects. The time-reversal method utilizes the time-reversal invariance of the wave equation by applying time inversion and phase conjugation to the received signal. This reconstructs the wavefield along its original path, focusing energy at the defect location. The core of this focusing effect lies in the fidelity of the inverted signal to the original wavefield information. Therefore, accurately extracting the echo segment containing the primary modal components and their relative time delay information from the received signal becomes the key factor determining detection sensitivity. Experiments employed a sine wave excitation source with a center frequency of 70 kHz and a 10-cycle Hanning window modulation. The L(0,2) mode guided wave was excited at the pipe end via the inverse piezoelectric effect. The response signal collected by the receiving array comprised three components: direct wave, defect-scattered wave, and end reflection wave. To systematically investigate the impact of window width on focusing effectiveness, rectangular windows of varying widths were applied to each channel signal while maintaining a fixed start time. After time-reversal processing, these signals were re-applied as secondary excitation signals to the corresponding excitation units. By superimposing responses from all receiving channels, time-reversed detection signals corresponding to different window widths were obtained, providing experimental basis for optimizing window width parameters.

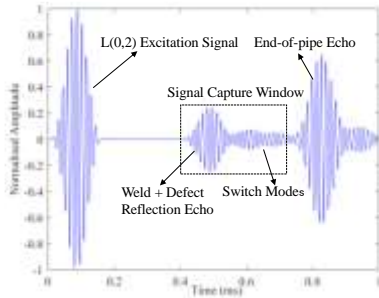
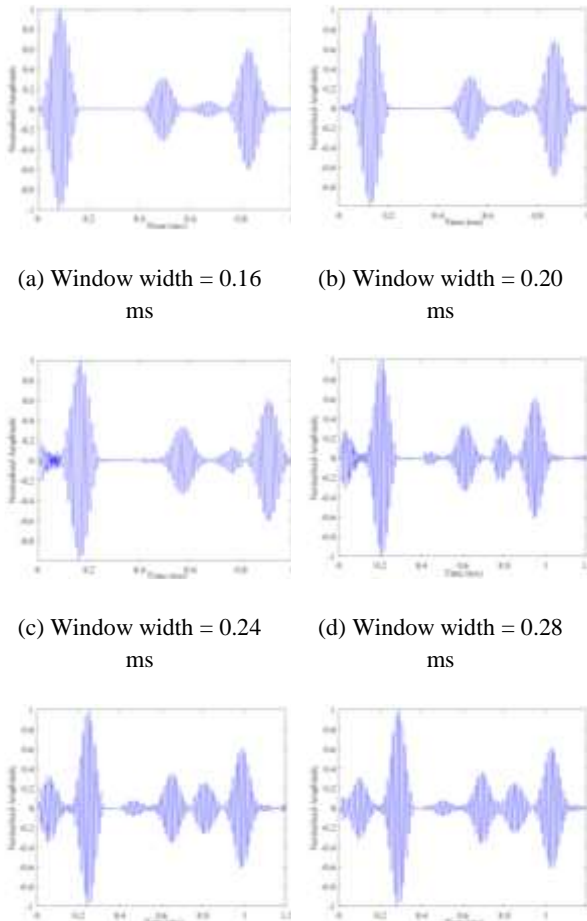


Fig.4 Direct Guided Wave Method for Monitoring Axial Time-History Signals at Individual Receiving Nodes

As the rectangular sampling window width increases from 0.16 mm to 0.32 mm, the amplitude of defect reflection echoes in the time-reversed detection signal grows accordingly, with a corresponding significant improvement in the defect reflection coefficient. This indicates a positive correlation between the sampling window width and the defect response intensity in the time-reversal method.



(e) Window width = 0.32 ms (f) Window width = 0.36 ms

Fig.5 Time reversal detection results with different interception windows

Monitoring using the time reversal method with window widths ranging from 0.16 to 0.36 ms showed the defect reflection coefficient gradually increasing from 0.3158 to 0.3653. Compared to the direct guided wave method (0.1474), the amplification factor increased from 2.141 times to 2.478 times. The results indicate that the intercept window width significantly influences the reflected echo amplitude, with their relationship curve shown in Figure 3-18.

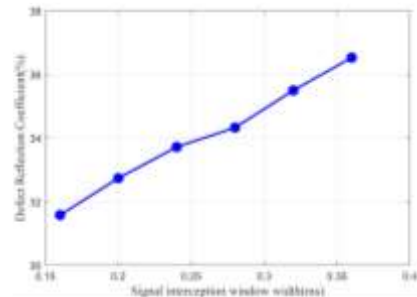


Fig. 6 Relationship curve between signal sampling window width and defect reflection coefficient

As shown in Fig. 3-11, in time-reversed guided wave detection, the defect reflection coefficient exhibits a clear positive correlation with the signal sampling window width. The underlying mechanism is that increasing the window width enables more complete capture of the multimodal conversion wave components excited by the defect. When these signals, containing richer modal information, undergo time reversal and re-excitation, the wavefield energy originally dispersed across different modes achieves more thorough spatiotemporal modulation and coherent superposition at the defect location. This significantly enhances the defect echo amplitude, thereby increasing the reflection coefficient. It is crucial to emphasize that to ensure effective energy focusing, the capture window must strictly exclude non-defect-related components such as the excitation signal segment and end reflections from the pipeline. This guarantees the specificity and accuracy of the time-reversed wavefield reconstruction.

2. ACKNOWLEDGMENTS

(1) Based on the time-reversal symmetry of the wave equation, the spatiotemporal focusing mechanism of time-reversed guided waves is elucidated. This method enables synchronous convergence of multimodal guided waves at the defect

location, achieving a defect reflection coefficient approximately 2.14 times higher than direct guided wave methods, providing a theoretical foundation for weld defect detection.

(2) The influence of window width on focusing performance was analyzed. Results indicate that increasing window width

enables more complete capture of multimodal information, elevating the defect reflection coefficient from 0.3158 to 0.3653 and boosting the enhancement factor from 2.141 to 2.478. Window width settings must avoid non-defect signals to ensure focusing accuracy.

(3) A pipeline weld defect detection model was established using COMSOL, with pipeline parameters of 2000 mm × ϕ 70 mm × 4 mm and a weld located at 1100 mm. A sensor array comprising 16 PZT elements was simulated, using the L(0,2) mode at 70 kHz as the excitation source, providing a simulation platform for subsequent analysis.

(4) yielded the relationship curve between window width and defect reflection coefficient. The two exhibit a positive correlation with gradually slowing growth, providing a basis for window width optimization in practical detection: appropriately increasing the window width while avoiding interference can enhance response intensity, but signal integrity and computational efficiency must be balanced. Our thanks to the experts who have contributed towards development of the template.

REFERENCES

- [1] Xu Z, Sampath S, Wang X, et al. Review on structural health monitoring of pipelines: from the perspective of acoustic-based crack detection [J]. *Measurement*, 2026, 263120075-120075. DOI: 10.1016/J.MEASUREMENT.2025.120075.
- [2] Yan Xia N, Long Xiang S, Xuan Y W, et al. New technology for pipeline defect detection[J]. *Science China (Technological Sciences)*, 2024, 67(04): 1294-1296.
- [3] Yu Z, Shan D, Sun R. State of the art for knowledge transfer in bridge structural health monitoring: Methodology, applications, and challenges[J]. *Measurement*, 2026, 262120008-120008. DOI:10.1016/J.MEASUREMENT.2025.120008.
- [4] JHaseeb A S, Krawczuk M. A State-of-the-Art Review of Structural Health Monitoring Techniques for Wind Turbine Blades[J]. *Journal of Nondestructive Evaluation*, 2025, 45(1):4-4. DOI:10.1007/S10921-025-01296-5.
- [5] Elsis A, Zamrawi A, Emad S. A Comprehensive Review of Structural Health Monitoring for Steel Bridges: Technologies, Data Analytics, and Future Directions[J]. *Applied Sciences*, 2025, 15(22): 12090.
- [6] Beena, K., Shruti, S., Sandeep, S., and Naveen, K. (2017). "Monitoring degradation in concrete-filled steel tubular sections using guided waves." *Smart Structures and Systems, International Journal*, 19(4), 371-382. <https://doi.org/10.12989/sss.2016.19.4.371>
- [7] Cahill, P., Pakrashi, V., and Sun, P. (2018), "Energy harvesting techniques for health monitoring and indicators for control of a damaged pipe structure," *Smart Struct. Syst., Int. J.*, 21(3), 287-303. <https://doi.org/10.12989/sss.2018.21.3.287>
- [8] Tang Y, Wan S, Yang Q, et al. A Review: Research Progress in Bridge Structural Health Monitoring From the Perspective of AI Development[J]. *Structural Control and Health Monitoring*, 2025, 2025(1): 8870840. DOI:10.1155/STC/8870840.
- [9] Almahakeri M, Mahasneh A J A, Mallouh A M, et al. Deep neural network based intelligent health monitoring system for oil and gas pipelines[J]. *Applied Soft Computing*, 2025, 171112827-112827. DOI:10.1016/J.ASOC.2025.112827.
- [10] Saleh N O, Jaber A A, Hussein M R. Applications of Structural Health Monitoring Approach for Defect Detection in Composite Structures: A Review of [J]. *Iranian Journal of Science and Technology, Transactions of Civil Engineering*, 2025, (prepublish): 1-30. DOI: 10.1007/S40996-025-02039-2.
- [11] Rose J L. *Ultrasonic Guided Waves in Solid Media*. Cambridge: Cambridge University Press, 2014.
- [12] Alleyne D N, Cawley P. A two-dimensional Fourier transform method for the measurement of propagating multimode signals. *Journal of the Acoustical Society of America*, 1991, 89(3): 1159–1168.
- [13] Lowe M J S, Alleyne D N, Cawley P. Defect detection in pipes using guided waves. *Ultrasonics*, 1998, 36(1–5): 147–154.
- [14] Wilcox P D. Guided wave inspection of large structures using permanently attached transducers. *Insight*, 2003, 45(3): 158–161.
- [15] Fink M. Time-reversed acoustics. *Physics Today*, 1997, 50(3): 34–40.
- [16] Prada C, Thomas J L, Fink M. The iterative time reversal process: analysis of the convergence. *Journal of the Acoustical Society of America*, 1991, 97(1): 62–71.
- [17] Michaels J E, Michaels T E. Guided wave signal processing and image fusion for in situ damage localization in plates. *Wave Motion*, 2007, 44(6): 482–492.
- [18] Giurgiutiu V. *Structural Health Monitoring with Piezoelectric Wafer Active Sensors*. Academic Press, 2008.